*Proc. Nat. Acad. Sci. USA*
Vol. 71, No. 7, pp. 2684–2688, July 1974

# Kinetics of the Crystalline–Liquid Crystalline Phase Transition of Dimyristoyl *L*-α-Lecithin Bilayers

**(lipid bilayer/temperature-jump)**

TIAN YOW TSONG

Department of Physiological Chemistry, The Johns Hopkins University School of Medicine, Baltimore, Maryland 21205

*Communicated by Albert L. Lehninger, April 16, 1974*

**ABSTRACT** **Aqueous dispersions of synthetic dimyristoyl *L*-α-lecithin undergo a sharp decrease in turbidity in the temperature range where the crystalline–liquid crystalline phase transition occurs. Equilibrium transition curves, monitored by the absorbancy change at 300 nm, reproduce all the important features of a calorimetric melting curve [Hinz & Sturtevant (1972) *J. Biol. Chem.* 247, 6071]. A rapid temperature-jump of the dispersion, measured by the same absorbancy change, has detected several different molecular processes depending on the magnitude of the perturbation. These processes include a phase transition, permeation of ions and water across the membrane, and rupture, annealing, or fusion of the bilayer structures. When the temperature-jump is limited to 1 degree, only reactions associated with the phase transition are detectable and no signal is generated after a temperature-jump except for those which end within or extend beyond the transition zones.**

**At least two relaxation times are resolved for the phase transition reactions. The faster one in the millisecond time range is strongly temperature-dependent and has an activation energy close to one million calories per mole. The second one, in the 100-msec time range, appears to have a much smaller activation energy. These observations indicate that strongly cooperative nucleation processes and energy-dependent fast propagation steps occur during the phase transition. Since the kinetics of the transition are complex, intermediate states or transient structures must exist in the transition regions of the bilayer dispersions. These thermal fluctuations of the bilayer structures may have important effects on the lateral diffusion and permeation of molecules and ions in the membrane structure.**

The dynamic properties of phospholipid bilayer structures are the focus of many recent publications (1–4). Especially important is the fact that the fluidity of the phospholipid bilayer structure changes dramatically in the temperature range where a crystalline–liquid crystalline phase transition occurs (5, 6). That such a phase transition of phospholipids exists in the naturally occurring biological membrane and in the living cell has been unequivocably demonstrated (7–9). The effects of this phase transition on the biological function of cell membrane are under intensive investigation.

Many equilibrium studies of the lipid phase transition have been published but direct kinetic measurement of the transition processes has not been as successful because any rapid thermal perturbation of the membrane suspension seems to induce a permeation of water or ions across the membrane (10, 11). Furthermore, the signals due to the permeation processes are difficult to separate from the signals coming from the phase transition reactions. We have employed the temperature-jump kinetic method of Eigen and deMaeyer (12) to study various relaxation phenomena in aqueous suspensions of artificial lipid bilayers and *Bacillus subtilis* membrane. Careful control of the magnitude of temperature-jump and a careful selection of temperature range for the kinetic experiments, makes it possible to separate several different molecular processes including ion permeations, rupture and fusion of bilayer structures, and the phase transition processes. We report here a kinetic study of the crystalline–liquid crystalline phase transition of the aqueous dispersion of dimyristoyl *L*-α-lecithin (DML).

A similar temperature-jump relaxation study of the phospholipid dispersions was reported by Träuble (13). He measured changes in the binding of bromothymol blue to the hydrophilic head groups of the dipalmitoyl *L*-α-lecithin (DPL) bilayers in the phase transition region and detected a single relaxation time. The van't Hoff ΔH and the activation energy obtained for these reactions are one order of magnitude smaller than the value we found for the crystalline–liquid crystalline phase transitions of the DML dispersions. Our kinetic results also appear to be more complex in that at least two relaxation times can be easily resolved. Hsu and Chan (14), using nuclear magnetic resonance spectroscopy, studied the equilibrium of the phase transitions of DML and DPL dispersions by investigating the binding of valinomycin to membranes and concluded that the binding occurred predominantly in the region of the polar head group.

## MATERIALS AND METHODS

Dimyristoyl *L*-α-lecithin (DML) lot no. 429475 and dipalmitoyl *L*-α-lecithin (DPL) lot no. 201409, purchased from Calbiochem, were used without further purification. Unsonicated lipid dispersions were prepared by mixing the phospholipids with 0.1 N NaCl and 0.05 M phosphate buffer at pH 7.0. The mixture was gently shaken at a temperature 5 degrees above the upper phase transition temperature ($T_{m2}$) for 5 min and kept at that temperature until used. Sonicated dispersions were prepared by sonic irradiation with a small probe in a Bronwill Biosonik model B10–11 at a 20% energy level for 30 min. During sonication the dispersions were maintained at a temperature several degrees below $T_{m2}$, and were kept at this same temperature until used.

Equilibrium melting curves were taken in a Zeiss spectrophotometer; cell temperature was programmed with a Neslab TP-2 temperature programmer and was monitored with a YSI thermoprobe. A higher heating rate (0.3 degree/min) was usually employed with unsonicated lipid dispersions since they settle slowly in the spectrophotometer cell. Manual reading

Abbreviations: DML, dimyristoyl *L*-α-lecithin; DPL, dipalmitoyl *L*-α-lecithin. 1 calorie = 4.184 joules.

was made with blank absorption and dark current adjusted for every point.

Rapid kinetic measurements were done with an Eigen-deMaeyer temperature-jump kinetic system. The solution temperature was measured with the same YSI probe by placing it into a hole in the upper electrode of the temperature-jump cell.

## RESULTS

### Equilibrium melting curves

Of the various physical properties used to follow the phase transition of the bilayer structure, the light scattering changes (as measured by the optical density changes) seem to be the most suitable for rapid kinetic measurement. Träuble and his coworkers demonstrated that the transition curves measured by the changes in 90° light scattering, absorbancy, fluorescence intensity of fluoroprobes, and an order parameter of spin labels (9), all exhibit the same characteristics. More recently, MacDonald and Yi (15) showed that the changes in absorbancy and light scattering of the dispersion can be quantitatively accounted for by the changes in refractive index and the anisotropy of the bilayer. The changes in refractive index is accounted for by the known expansion and corresponding decrease in density of the lipid bilayer structure. This being the case, it is still important to compare the transition curves obtained by direct absorbancy measurement with those obtained by a precise microcalorimetric measurement.

Fig. 1 gives two thermal transition curves, measured by the absorbancy change at 300 nm, for an unsonicated and a sonicated DML dispersions. As can be seen, the transition curves reproduce all the important features of a microcalorimetric curve (6) including lower and upper transition points, and an extremely sharp slope at the mid-point of the upper transition. Some numerical values characteristic of these transition curves are listed in Table 1 and are in good agreement with the results of Hinz and Sturtevant (6).

In Table 1 the van't Hoff $\Delta H(\Delta H_{vH})$ is calculated according to the relation $\Delta H_{vH}(T_m) = 4RT_m^2(d\theta/dT)_{T=T_m}$, in which $(d\theta/dT)_{T=T_m}$ is the slope of the transition at transition mid-point $T_m$. The cooperative unit, which is the ratio of $\Delta H_{vH}$ to $\Delta H$ values actually measured by microcalorimetry [i.e., 6.26 kcal/mole of monomer for the upper transition and 1.1 kcal/mole of monomer for the lower transition (6)], represents the lower limit of the number of molecules involved as a unit in the cooperative transition (6, 8).

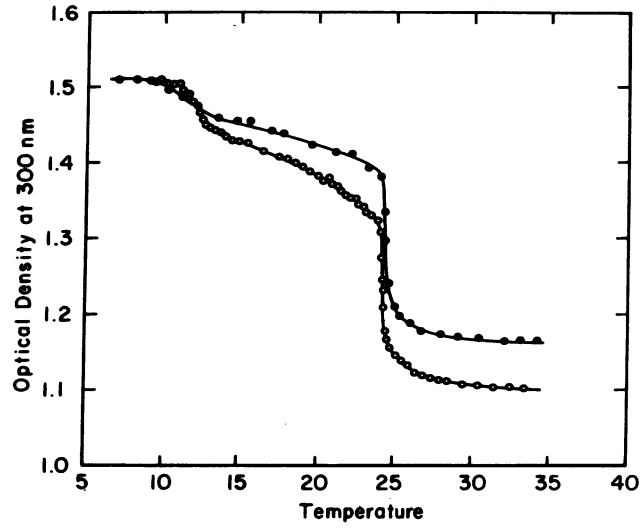


FIG. 1. Equilibrium crystalline–liquid crystalline phase transition curves of *L*-α-lecithin (β-*r*-dimyristoyl). ●, 0.5 mg/ml of unsonicated dispersion, heating rate 0.30 degree/min; ○, 0.85 mg/ml of sonicated dispersion, heating rate 0.18 degree/min. Conditions: 0.10 N NaCl, 0.05 M phosphate buffer at pH 7.0.

### Kinetics of the crystalline–liquid crystalline phase transition

Since the optical density change associated with the upper transitions (Fig. 1) is huge, and the transition process is nearly isothermal, a minute temperature-jump inside the transition region should induce a sizeable absorbancy change. We have consistently been using a jump of <0.3 degrees in temperature to study the kinetics of the upper phase transitions. Under such conditions, no signal is generated after a temperature-jump except for those which end within or extend beyond the transition zones. To obtain a measurable signal for the lower transition, a larger temperature perturbation is required. However, a limit of 1 degree has to be set since a perturbation size of about 3 degrees generates a signal at any

TABLE 1. *Some numerical values for the crystalline–liquid crystalline phase transition of aqueous dispersion of dimyristoyl L-α-lecithin*

| | Lower transition | | | | Upper transition | | | |
|---|---|---|---|---|---|---|---|---|
| Measurements | $T_{m1}$ °C | $\left(\frac{d\theta}{dT}\right)$ $T = T_{m1}$ deg$^{-1}$ | $\Delta H_{vH}$ $(T_{m1})$ $10^6$ cal | cooperative unit molecules | $T_{m2}$ °C | $\left(\frac{d\theta}{dT}\right)$ $T = T_{m2}$ deg$^{-1}$ | $\Delta H_{vH}$ $(T_{m2})$ $10^6$ cal | cooperative unit molecules |
| Sonicated sample | | | | | | | | |
| Equilibrium* | 12.5 | 0.40 | 0.26 | 240 | 24.1 | 2.1 | 1.5 | 240 |
| Kinetic† | — | — | — | — | 23.8 | 2.2 | 1.55 | 250 |
| Unsonicated sample | | | | | | | | |
| Equilibrium* | 12.0 | 0.35 | 0.23 | 210 | 24.2 | 2.0 | 1.4 | 220 |
| Kinetic† | — | — | — | — | 24.1 | 2.2 | 1.55 | 250 |
| Calorimetric‡ | 13.5 ± 0.2 | — | — | 200 ± 40 | 23.7 ± 0.09 | — | — | 200 ± 40 |

Conditions: 0.10 N NaCl, 0.05 M phosphate buffer at pH 7.0.

* Data from Fig. 1.

† $(d\theta/dT)_{T=T_m}$ taken from Fig. 3.

‡ Data of Hinz and Sturtevant (6).

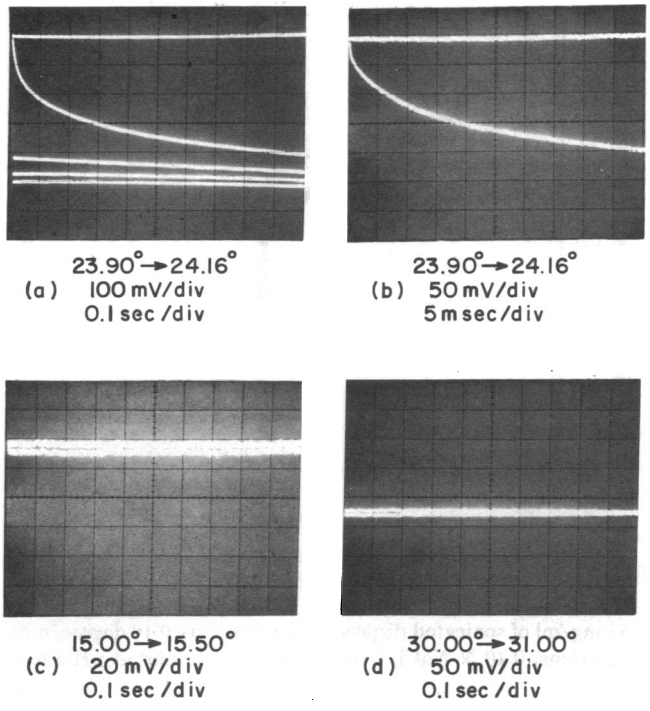


FIG. 2. Oscilloscope record of the temperature-jump kinetic measurements of the sonicated DML dispersion. *Upper curves* in each picture represent signal positions before jumps. *Lower curves* indicate the kinetics of the transitions. (*a*) and (*b*), a 0.26 degree-jump inside the upper phase transition; (*c*) and (*d*), jumps outside of the transition generate no measurable signals. Conditions: 2 mg DML/ml, 0.10 N NaCl, 0.05 M phosphate buffer at pH 7.0. Kinetics measured by absorbancy changes at 300 nm.

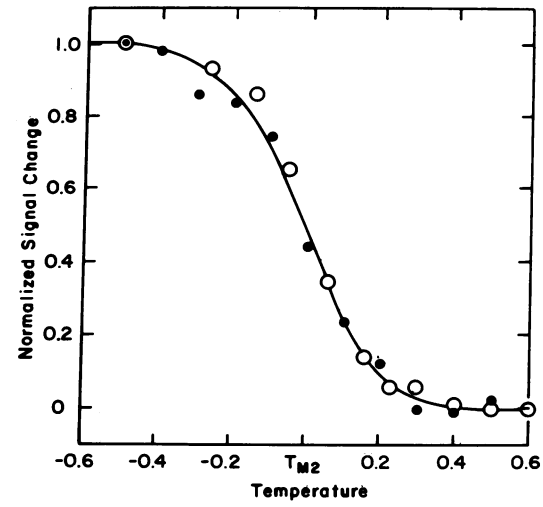


FIG. 3. Kinetic melting curve of the upper transition shown in Fig. 1. The temperatures of the dispersions (○, sonicated; ●, unsonicated) were kept at about 0.5 degree below the mid-point of the upper transition. Varied temperature-jumps, from 0.1 degree to 1.1 degree, were then applied to the dispersions. The signals so generated are plotted against the jump sizes. In the plot, the signals are normalized to unit values for the 1.1 degree-jump. For details see the *text*. Conditions are as given in Fig. 2.

temperature range studied. In Fig. 2, several oscilloscope records of the kinetics of the phase transition are shown.

To demonstrate further that the signals measured under these conditions do detect the phase transition of the lipid dispersions, we kept the temperature of the dispersion constant at the entrance of the upper transition, and used different temperature-jump sizes, ranging from 0.1 degree of 1.1 degree, across the transition zones. The signals so generated were then plotted against the jump size. Thus, a kinetic transition curve could be constructed. The $T_{m2}$ values, so obtained, are 23.8°C and 24.1°C, respectively, for a sonicated and an unsonicated dispersion. When the two transition mid-points are superimposed, the $\Delta H_{vH}$ values calculated from the curve (Fig. 3) agree with those obtained in the equilibrium measurements (Table 1).

At least two relaxation times are resolved for the kinetics of the phase transition. The faster one ($\tau_2$*) in the millisecond time range is strongly temperature-dependent, whereas the slower one ($\tau_1$) in the 100-msec time range appears to be much less temperature-dependent (Table 2, Fig. 4). Both relaxation times are independent of the perturbation size (within 1 degree limit), and are a function only of the temperature. Both relaxation times are also independent of the electric field intensity pulsating across the solutions (from 5 kV/cm to 30 kV/cm), suggesting that the reactions are purely thermal

TABLE 2. *Fast temperature-jump measurement of the crystalline–liquid crystalline phase transition of dimyristoyl L-α-lecithin (jump size 0.1 ~ 0.8 deg)*

| Sonicated dispersion | | | | | Unsonicated dispersion | | | | |
|---|---|---|---|---|---|---|---|---|---|
| Final temperature | $\tau_1$ sec | $\tau_2$* msec | $\alpha_1$ % | $\alpha_2$ % | Final temperature | $\tau_1$ sec | $\tau_2$* msec | $\alpha_1$ % | $\alpha_2$ % |
| 13.40 | 0.19 | <0.005 | 25 | 75 | 23.90 | 0.74 | 11 | 59 | 41 |
| 24.16 | 1.58 | 10 | 50 | 50 | 24.00 | 0.81 | 7.8 | 50 | 50 |
| 24.24 | 1.15 | 8.2 | 36 | 64 | 24.10 | 0.66 | 5.0 | 50 | 50 |
| 24.30 | 1.22 | 6.1 | 33 | 67 | 24.20 | 0.53 | 2.9 | 52 | 48 |
| 24.40 | 1.24 | 4.0 | 21 | 89 | 24.30 | 0.64 | 1.1 | 48 | 50 |
| 24.50 | — | 3.1 | Small | >95 | 24.40 | 0.75 | 0.78 | 42 | 58 |
| 24.60 | — | 1.6 | Small | >95 | 24.50 | 0.65 | 0.43 | 37 | 63 |
| 24.70 | — | 1.0 | Small | >95 | 24.60 | — | 0.38 | — | — |
| 24.80 | — | 0.65 | Small | >95 | 24.90 | — | 0.16 | — | — |
| 25.00 | — | 0.40 | Small | >95 | 25.00 | — | 0.072 | — | — |

Conditions: 2 mg/ml of DML in 0.1 N NaCl, 0.05 M phosphate buffer at pH 7.0. $\tau_2$* is the mean relaxation time as defined by Schwarz (22). In estimating $\alpha_1$ and $\alpha_2$, the amplitudes of signal change occurring in the slower and faster kinetic phases respectively, it was assumed that there was no significant contribution from reactions slower than $\tau_1$.

in nature. The relative amplitudes of the fast relaxation ($\alpha_2$) and the slow relaxation ($\alpha_1$), however, depend on the perturbation size. This is expected if the fast reaction represents a transient phase and the slow reaction represents a steady-state phase of a nucleation-dependent kinetic model (16, 17).

The kinetic behavior of sonicated and unsonicated samples appears to be slightly different. Both the fast and the slow relaxation times are smaller in the unsonicated sample. The kinetics of the sonicated dispersion is dominated by the fast phase ($\tau_2$*) in the second half of the transition. In contrast, the slow reaction continues to occur in the entire transition zone of the unsonicated dispersion. Although the differences in kinetic complexity of the two samples could simply reflect differences in heterogeneity of size distributions, this may not be so since the relative amplitudes of the slow and the fast reactions depend also on the perturbation size. It seems plausible that the kinetic differences may actually reflect a subtle variation in the bilayer arrangements of the two dispersions (18).

The most striking result of these kinetic measurements is that the activation energy of the fast reaction is extremely large, approaching one million calories/mole (see *legend* for Fig. 4). The rate increases nearly 80-fold within 1 degree. This finding is consistent with the equilibrium observation that the van't Hoff $\Delta H$ of the transition curves has values near one and a half million calories/mole (Table 1). However, the slower reactions are much less sensitive to the temperature change. The small slope of the Arrhenius plots for the slower reactions ($\tau_1$) in Fig. 4 does not necessarily mean that the activation energy of the slow relaxation is zero, since the temperature range shown in the plots spans less than 1 degree. In any case, the highly cooperative nature of the bilayer phase transition is obvious.

It would be interesting to study the kinetics of the lipid phase transition in a homogeneous vesicle system such as that described by Huang (19). However, we have found that the Huang's vesicles are stable only at temperatures below the phase transition region. The homogeneity of the vesicles as indicated by Sepharose chromatography is even more difficult to maintain when 0.1 N NaCl is present (18). The presence of such a salt concentration is essential for our temperature-jump experiment. Nevertheless, the vesicle preparation of Huang can provide an interesting model system for studying the rupture and fusion of the membrane structures. We have evidence suggesting that such reactions exist in the vesicle suspension when a large temperature jump is applied to the suspension.

## CONCLUSION

X-Ray and other physical studies show that below the transition, the hydrocarbon chains of phospholipids exist in a hexagonal, closely packed, gel phase. The phase transitions promote the motional freedom of the hydrocarbon chains (20, 21), and are accompanied by a substantial increase in the partial molal volume of the bilayer structures (18). Living cells do grow within the phase transition regions of phospholipids in the membranes (7, 8). The mechanisms and the time course of the transitions should influence our understanding of the membrane functions. Data reported in this communication do not permit us to formulate a definite kinetic scheme (see *legend* for Fig. 4). Nevertheless, they clearly demonstrate that the transitions are highly cooperative, and the rate of these transitions are surprisingly slow. *Consequently, it is clear that intermediate stages or transient structures exist in the transition regions of bilayer dispersions.* Whether these thermal fluctuations of the bilayer structures actually provide driving forces for biologically important processes such as the lateral diffusion of protein particles on the membrane surface and transport of various molecules across the membrane remains to be seen.[a]

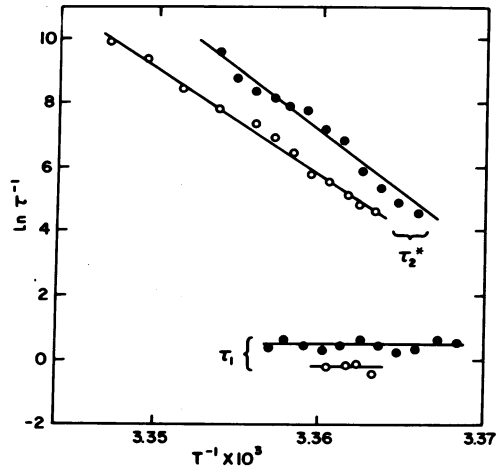


FIG. 4. Temperature variation of the slow ($\tau_1$) and the fast ($\tau_2$*) relaxation times. The kinetics may be understood through a simplified two step model.

$$A_1 \underset{k_{21}}{\overset{k_{12}}{\rightleftharpoons}} A_2 \underset{k_{32}}{\overset{k_{23}}{\rightleftharpoons}} A_3$$

The first step is a nucleation event in which a minimum number of the hydrocarbon chains is required to start the phase transitions. The nucleation may occur at *lattice defect* sites or *void lattices* of the bilayer stuctures. The second step represents a series of propagation reactions. Under these assumptions it can be shown that

$$\frac{1}{\tau_1} = k_{12} + \frac{k_{21}}{1 + K_{23}}, \qquad \text{where } K_{23} = \frac{(A_3)}{(A_2)}$$

and

$$\frac{1}{\tau_2^*} = k_{23} + k_{32}.$$

At the top of the transition, $(A_3) \gg (A_2)$

hence

$$\frac{1}{\tau_2^*} \sim k_{23}.$$

The Arrhenius plots for the fast reactions indicate that $k_{23}$ is the step(s) which involve(s) a large activation energy. The activation energy of the fast reaction for the sonicated dispersions (○) is $0.66 \times 10^6$ calorie/mole and for the unsonicated dispersions (●) is $0.77 \times 10^6$ calorie/mole.

[a] Assuming that the actual cooperative unit of the phase transition is around 400 monomers per mole and that the phase transition traverses at the speed measured by the $\tau_2$* (which is the relaxation time of the propagation reactions), then the transition covering a surface area $A$ per second is $\Delta A/\Delta t \sim 400a/2\tau_2$*, where $a$ is the area occupied per monomer. If $a$ = 48 Å$^2$ and 58 Å$^2$, and $\tau_2$* = 20 and 0.1 msec, respectively, for the bilayer at the beginning and at the end of the transition, then $\Delta A/\Delta t \sim 6 \times 10^{-11}$ cm$^2$/sec at the entrance and $1.2 \times 10^{-8}$ cm$^2$/sec at the top of the transition. Träuble and Sackmann (23), using electron spin resonance estimated that the translational diffusion coefficient of the steroid molecules within the DPL lipid matrix above the $T_{m2}$ is about $1 \times 10^{-8}$ cm$^2$/sec.

Recently, Shimshick and McConnell (24) and Wu and McConnell (25) reported very interesting studies of the lateral phase separations in mixed phospholipid bilayers. They observed that within a certain temperature range the gel phase (S state) and the liquid crystalline phase (F state) of the lipid constituents can separate and coexist. This coexistence can provide a high lateral compressibility and extensibility which in turn can facilitate the insertion and transport of protein molecules in the membrane structures. Papahadjopoulos *et al.* (26) studied the temperature dependence of the $^{22}Na^+$ permeation through the membrane vesicles and suggested that the boundary regions of the solid and liquid crystalline phases may exhibit greater permeability to the $^{22}Na^+$ ions. Our observation of the highly cooperative and complex kinetics for the phase transition of a single component lipid system extends these concepts further in that such regulatory mechanisms of the membrane structures may indeed exist, even in a pure lipid system. Detection of the transient structures in the phase transition region also deserves further attention.

The author is indebted to Dr. W. Lennarz for many stimulating discussions, and to Ms. M. Kennedy and S. Krag for *B. subtilis* membrane preparations. This work is supported by NSF Grant no. GB 38374.

1. Hubbell, W. L. & McConnell, H. M. (1968) *Proc. Nat. Acad. Sci. USA* **61**, 12–16.
2. Singer, S. J. & Nicolson, G. L. (1972) *Science* **175**, 720–731.
3. Devaux, P. & McConnell, H. M. (1972) *J. Amer. Chem. Soc.* **94**, 4475–4481.
4. Sackmann, E., Träuble, H., Galla, H.-J. & Overath, P. (1973) *Biochemistry* **12**, 5360–5369.
5. Barratt, M. D., Green, D. K. & Chapman, D. (1969) *Chem. Phys. Lipids* **3**, 140–144.
6. Hinz, H.-J. & Sturtevant, J. (1972) *J. Biol. Chem.* **247**, 6071–6075.
7. Reinert, J. C. & Steim, J. M. (1970) *Science* **168**, 1580–1582.
8. Melchior, D. L., Morowitz, H. J., Sturtevant, J. M. & Tsong, T. Y. (1970) *Biochim. Biophys. Acta* **219**, 114–122.
9. Overath, P. & Träuble, H. (1973) *Biochemistry* **12**, 2625–2634.
10. Owen, J. D., Bennion, B. C., Holmes, L. P., Eyring, E. M., Berg, M. W. & Lords, J. L. (1970) *Biochim. Biophys. Acta* **203**, 77–82.
11. Owen, J. D., Hemmes, P. & Eyring, E. M. (1970) *Biochim. Biophys. Acta* **219**, 276–282.
12. Eigen, M. & deMaeyer, L. C. (1963) *Techniques of Organic Chemistry*, eds. Freiss, S. L., Lewis, E. S. & Weissberger, A. (Interscience Publishers, New York), Vol. 8, part II, pp. 845–1054.
13. Träuble, H. (1971) *Naturwissenschaften* **58**, 277–284.
14. Hsu, M. & Chan, S. I. (1973) *Biochemistry* **12**, 3872–3876.
15. Yi, P. N. & MacDonald, R. C. (1973) *Chem. Phys. Lipids* **11**, 114–134.
16. Tsong, T. Y., Baldwin, R. L., McPhie, P. & Elson, E. L. (1972) *J. Mol. Biol.* **63**, 453–475.
17. Elson, E. L. (1972) *Biopolymers* **11**, 1499–1520.
18. Sheetz, M. P. & Chan, S. I. (1972) *Biochemistry* **11**, 4573–4581.
19. Huang, C. (1969) *Biochemistry* **8**, 344–352.
20. Ladbrook, B. D. & Chapman, D. (1969) *Chem. Phys. Lipids* **3**, 304–356.
21. Chapman, D., Williams, R. M. & Ladbrook, B. B. (1967) *Chem. Phys. Lipids* **1**, 445–475.
22. Schwarz, G. (1965) *J. Mol. Biol.* **11**, 64–77.
23. Träuble, H. & Sackmann, E. (1972) *J. Amer. Chem. Soc.* **94**, 4499–4510.
24. Shimshick, E. J. & McConnell, H. M. (1973) *Biochemistry* **12**, 2351–2360.
25. Wu, S. H. & McConnell, H. M. (1973) *Biochem. Biophys. Res. Commun.* **55**, 484–491.
26. Papahadjopoulos, D., Jacobson, K., Nir, S. & Isac, T. (1973) *Biochim. Biophys. Acta* **311**, 330–348.